

Sturmian-Floquet approach to high-order harmonic generation

József Kasza,¹ Péter Dombi,^{1,2} and Péter Földi^{1,3}

¹*ELI-ALPS, ELI-HU Non-profit Ltd., Dugonics tér 13, H-6720 Szeged, Hungary**

²*MTA "Lendület" Ultrafast Nanooptics Group, Wigner Research Center for Physics, Konkoly-Thege Miklós út 29-33, H-1121 Budapest, Hungary*

³*Department of Theoretical Physics, University of Szeged, Tisza Lajos körút 84, H-6720 Szeged, Hungary*

We show that the Floquet approach with a Sturmian basis means an efficient description of high-order harmonic generation with monochromatic excitation. This method, although involves numerical calculations, is close to analytic approaches with the corresponding deeper insight into the dynamics. As a first application, we investigate the role of atomic coherence during the process of HHG: as it is shown, different coherent superpositions of initial atomic states produce observably different HHG spectra. For linearly polarized excitation, we demonstrate that the question whether the constituents of the initial superpositions are dipole coupled or not, strongly influences the dynamics. By investigating time-dependent HHG signals, we also show that the preparation of the initial atomic state can be used for the control of the high-harmonic radiation.

PACS numbers:

I. INTRODUCTION

High-order harmonic generation (HHG) is a key concept in the recent development of optics, partially because of its fundamental aspects that can deepen our knowledge on nonlinear light-matter interaction [1], but also because of its importance in producing short, attosecond range bursts of electromagnetic radiation [2, 3]. This process was first observed for the case of gas samples [4, 5], but since the beginning of the 90's, a wide variety of physical systems were shown or predicted to produce high harmonics, including plasma surfaces [6–9], bulk solids [10] and nanostructures [11].

In the current paper, we focus on the interaction of short, intense laser fields and hydrogen-like atoms. In this context, the light-induced dynamics of the electrons naturally involve the continuum part of the spectrum, since the strong electromagnetic field of the laser can induce an ionization process, i.e., it can transfer the electrons to the continuum. In more detail, the most often used, so-called "three-step" model [12–14] consists of the emission of a single active electron, its motion "outside the atom", in the laser field, and recombination with the parent ion. This model, besides providing and instructive theoretical interpretation, can describe the main features of the gas HHG spectra.

The full quantum mechanical description of the process of HHG from gas samples means the solution of the corresponding time-dependent Schrödinger equation (TDSE) [15]. There are various numerical methods for this purpose, having an important point in common: the truncation of the underlying Hilbert-space. For discretization in real space, it means using a sufficiently large, but necessarily finite computational box, in order to avoid unphysical reflections at the boundaries. As a different

approximation, we can try to use a finite set of the hydrogenic eigenstates to describe the problem, or, as an intermediate way, can discretize in the radial direction, and use spherical harmonic expansion [14] for the remaining two dimensions.

For sinusoidally oscillating external fields, Floquet's method [16, 17] offers a convenient way to transfer the TDSE to a static eigenvalue problem. (Also for solid states systems, see e.g. [18, 19].) Numerically necessary truncation in this case means ignoring harmonics above a given order. Recalling the typical properties of gas HHG spectra (plateau and then a cutoff for increasing frequencies), this approximation can safely be performed, numerical errors can be kept under a predefined limit. The power and transparency of this method is most obvious when not too many quantum mechanical states have to be used to describe the time-dependent problem.

However, since a realistic description of the HHG process should involve the continuum as well, usual hydrogen-like eigenstates are not adequate. Instead, we use appropriate Sturmian functions [20, 21], which cover both the bound and the continuum part of the spectrum, and provide an appropriate basis. As we show, the combination of the Floquet approach with a Sturmian basis [22] means a method which is close to analytic approaches with the corresponding deeper insight into the dynamics. As a first application, we calculate HHG spectra for various laser parameters. We pay special attention to the initial atomic state, consider various superpositions of low-lying energy eigenstates [23]. As we show, atomic coherence has strong influence on the HHG signals, and this effect can be used for the optimization of attosecond pulse generation.

In the following, first we introduce the theoretical framework, Floquet's method and the Sturmian basis in Sec. II. We describe our results in Sec. III and draw the conclusions in Sec. IV.

*Electronic address: Jozsef.Kasza@eli-alps.hu

II. FLOQUET APPROACH AND STURMIAN FUNCTIONS

The time dependent Schrödinger equation that we consider reads:

$$i\hbar \frac{d}{dt} |\psi\rangle(t) = [H_0 + V(t)] |\psi\rangle(t), \quad (1)$$

where H_0 corresponds to the free atomic system (kinetic term plus the Coulomb potential). The interaction with a linearly polarized, monochromatic external laser field \mathbf{E} is given by

$$V(t) = \mathbf{D}\mathbf{E}_0 \cos(\omega t), \quad (2)$$

where \mathbf{D} is the dipole moment operator and \mathbf{E}_0 is assumed to be parallel with the x axis.

Since the Hamiltonian appearing in Eq. (1) is periodic in time ($T = 2\pi/\omega$), the infinite set of Floquet states

$$|\phi_k\rangle(t) = e^{i\epsilon_k t} |u_k\rangle(t) \quad (3)$$

with $|u_k\rangle(t+T) = |u_k\rangle(t)$ exists, and plays an important role in the theoretical description of the problem. Specifically, since the states $|\phi_k\rangle$ with $k = 0, 1, 2, \dots$ form a proper basis for all values of t , when the expansion

$$|\psi\rangle(0) = \sum_k c_k |\phi_k\rangle(0) = \sum_k c_k |u_k\rangle(0) \quad (4)$$

of an initial state is known, its time evolution can be calculated as simply as

$$|\psi\rangle(t) = \sum_k c_k |\phi_k\rangle(t) = \sum_k c_k e^{i\epsilon_k t} |u_k\rangle(t). \quad (5)$$

That is, having determined the Floquet quasienergies ϵ_k and the corresponding time-periodic states $|u_k\rangle(t)$, we essentially know the dynamics of any initial state.

Practically, ϵ_k and $|u_k\rangle(t)$ can be found using a set of orthogonal functions in real space (like, e.g., the usual hydrogenic eigenstates, $|n, l, m\rangle$) and considering Fourier functions $e^{ik\omega t}$ as a time domain basis for the periodic functions (with k being an integer). Using spherical coordinates, we can define

$$|n, l, m; k\rangle(\mathbf{r}, t) = |n, l, m\rangle(\mathbf{r}) e^{ik\omega t} = 2^{l+1} e^{-\frac{r}{a_0 n}} \left(\frac{r}{a_0 n} \right)^l \times \sqrt{\frac{(-l+n-1)!}{a_0^3 n^4 (l+n)!}} L_{-l+n-1}^{2l+1} \left(\frac{2r}{a_0 n} \right) Y_l^m(\theta, \phi) e^{ik\omega t}, \quad (6)$$

where L and Y denote associated Laguerre polynomials and the spherical harmonics, respectively. For the sake of simplicity, in the following the arguments (\mathbf{r}, t) will not appear explicitly in the notation, unless it is necessary. The states above are orthogonal in terms of the inner product

$$\langle \varphi_1 | \varphi_2 \rangle = \int_0^T dt \int_{-\infty}^{\infty} d^3 \mathbf{r} \varphi_1^*(\mathbf{r}, t) \varphi_2(\mathbf{r}, t), \quad (7)$$

that is, $\langle n, l, m; k | n', l', m'; k' \rangle = \delta_{nn'} \delta_{ll'} \delta_{mm'} \delta_{kk'}$. Using Eq. (3), the Floquet states can be searched in the following form:

$$|\phi_k\rangle(t) = \exp(i\epsilon_k t) \sum_{nlm} c_{nlm}^k |n, l, m; k\rangle(t). \quad (8)$$

Substituting this form back to the time dependent Schrödinger equation (1), and multiplying the result from the left by $\langle n', l', m'; k' |$, we obtain;

$$\epsilon_{k'} c_{n'l'm'}^{k'} = \sum_{nlm} c_{nlm}^k \langle n', l', m'; k' | H | n, l, m; k \rangle + k\omega \delta_{nn'} \delta_{ll'} \delta_{mm'} \delta_{kk'}. \quad (9)$$

By denoting all the four discrete indices (n, l, m, k) by a single integer variable j , and introducing $\tilde{H}_{jj'} = \langle n', l', m'; k' | H | n, l, m; k \rangle + k\omega \delta_{nn'} \delta_{ll'} \delta_{mm'} \delta_{kk'}$, Eq. (9) is seen to have the form of an eigenvalue equation:

$$\epsilon_j c_j = \sum_{j'} c_{j'} \langle j | \tilde{H} | j' \rangle. \quad (10)$$

(Note that here, if j corresponds to the indices (n, l, m, k) , c_j means c_{nlm}^k and ϵ_j denotes ϵ_k .) The matrix elements appearing above can be determined using the coordinate representation of the Hamiltonian $H(t)$ as well as the states $|n, l, m; k\rangle$ as given by Eq. (6). Clearly, we have

$$\langle n', l', m'; k' | H_0 | n, l, m; k \rangle = \frac{\mathcal{E}_0}{n^2} \delta_{nn'} \delta_{ll'} \delta_{mm'} \delta_{kk'}, \quad (11)$$

where $\mathcal{E}_0 = -1Ry \approx -13.6\text{eV}$ for the hydrogen atom. The interaction term $V(t)$ has explicit time dependence, and consequently will not be diagonal in the (time-related) last index:

$$\begin{aligned} \mathbf{D}\mathbf{E}_0 \cos(\omega t) |n, l, m; k\rangle &= \frac{E_0}{2} D (e^{i\omega t} + e^{-i\omega t}) |n, l, m; k\rangle \\ &= \frac{E_0}{2} D [|n, l, m; k+1\rangle + |n, l, m; k-1\rangle], \end{aligned} \quad (12)$$

where D means the x component of the \mathbf{D} operator. The spatial part of $V_{jj'}$ is determined by the usual dipole moment matrix elements.

Using Eqs. (11) and (12), we obtain an eigenvalue equation (10) with a known, infinite matrix \tilde{H} . For practical calculations – like in all numerical models – we have to truncate this matrix, and use a sufficiently large, but finite part of it, which is determined by the initial state as well as the strength of the laser-atom interaction (that is characterized by E_0). States corresponding to the “static” eigenfunctions $|n, l, m\rangle = |n, l, m; k=0\rangle$ should necessarily be taken into account. The number of nonzero k values (that are directly related to the high harmonics) playing an important role in the time evolution, depends on E_0 . (E.g., for a weak excitation corresponding to linear response, $k = \pm 1$ suffices.) From the experimental point of view, the initial states $|\psi\rangle(0)$ that

can be prepared in the most straightforward manner are the hydrogen-like bound states $|n, l, m\rangle$ or dipole coupled superpositions of them. Since generally downward transitions $n \rightarrow n' < n$ cannot be excluded, the ground state $|n = 1, l = 0, m = 0\rangle$ always has to be taken into account. As a rule of thumb, the highest the initial value of n is, the more elements of the numerically necessary finite basis has (and the problem is numerically more expensive to solve).

On the other hand, we have to recall, that hydrogen-like bound states $|n, l, m\rangle$, which are orthogonal to the positive-energy states in the continuum, does not form a complete basis. Additionally, the usual picture of the process of HHG in gas samples (emission of an electron, its motion in the laser field and recombination with the parent ion with the emission of the energy that were gained during this process as high harmonic radiation) strongly involves the continuum. Therefore, in order to describe the problem appropriately, we have to use a different set of spatial functions. The Sturmian states [24], the elements of which in coordinate representation can be written as

$$|S_{n,l,m}^\alpha\rangle(r, \theta, \phi) = \frac{\alpha^{3/2} 2^{l+1} e^{-\alpha r}}{(2l+1)!} \sqrt{\frac{(l+n)!}{n(-l+n-1)!}} \quad (13)$$

$$\times (\alpha r)^l {}_1F_1(l-n+1; 2l+2; 2\alpha r) Y_l^m(\theta, \phi)$$

form a basis in the space of normalizable states for all values of α (we use $\alpha = 1$), meaning an optimal choice for a norm-preserving, unitary dynamics that involves the continuum as well. By multiplying $|S_{n,l,m}^\alpha\rangle$ by $e^{ik\omega t}$, we obtain an analogue of the states $|n, l, m; k\rangle$ that is suitable for the description of the process of HHG. All the machinery described for $|n, l, m; k\rangle$ can be repeated also for $|S_{n,l,m}^\alpha\rangle e^{ik\omega t}$, but we have to keep in mind that the orthogonality relation for the Sturmian functions involves a weight function of $1/r$ [24, 25], thus the inner product (7) has to be replaced by

$$\langle \varphi_1 | \varphi_2 \rangle = \int dt \int \frac{1}{r} d^3\mathbf{r} \varphi_1^*(\mathbf{r}, t) \varphi_2(\mathbf{r}, t), \quad (14)$$

and the matrix elements of H_0 and $V(t)$ has to be evaluated using this inner product.

III. RESULTS

Although the dynamics of HHG is conveniently described using the Sturmian states (13), the initial states appearing in Eq. (4) that can most easily prepared by conventional, long, (almost) resonant pulses are energy eigenstates, or dipole coupled superpositions of them. For the sake of simplicity, in the following we consider

$$|\psi\rangle(0) = \cos\beta |n = 1, l = 0, m = 0\rangle + e^{i\delta} \sin\beta |n' = 2, l' = 1, m' = -1\rangle, \quad (15)$$

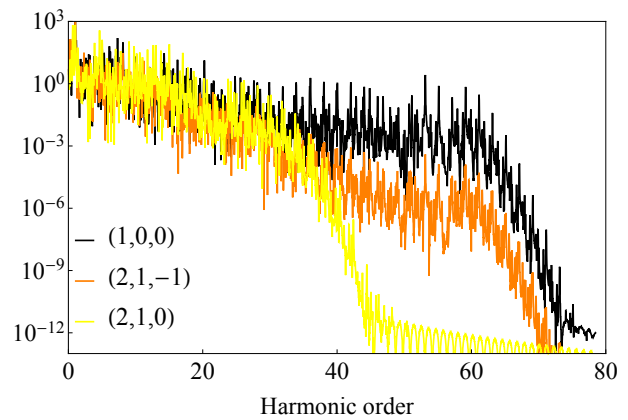


FIG. 1: HHG spectra for different initial states $|n, l, m\rangle$. The quantum numbers are indicated in the legend. The excitation is assumed to be monochromatic, with $E_0 = 0.1 a.u.$ and $\omega = 0.057 a.u.$ (which corresponds to $\lambda = 800 nm$).

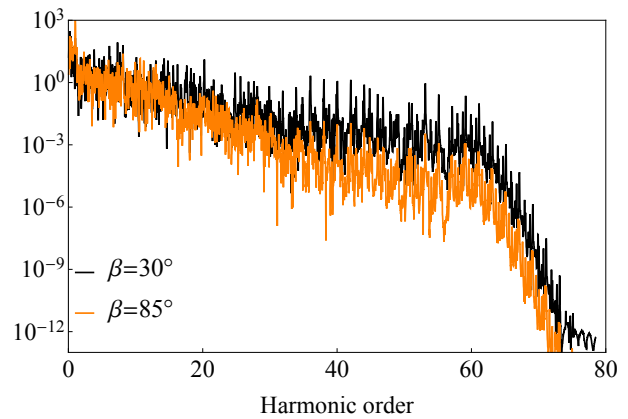


FIG. 2: HHG spectra for initial superpositions $\cos\beta |n = 1, l = 0, m = 0\rangle + \sin\beta |n' = 2, l' = 1, m' = -1\rangle$ for different values of β . The parameters of the exciting field are the same as in Fig. 1.

where $m' = 0, \pm 1$. Note that the case of $\beta = 0$ ($\pi/2$) means pure initial energy eigenstates. When β equals none of these values, we have a superposition of the ground state and an excited state, with a quantum mechanical phase given by δ . Additionally, when $m' = 0$, selection rules tell us that the external field that is polarized in the x direction, cannot induce dipole transitions between the constituents of the initial superpositions, while for $m' = \pm 1$, this transition is dipole-allowed. (Note that in order to prepare a superpositions with $m' = 0$ in Eq. (15), one can use a pulse polarized along the z axis.)

First, let us consider the case when, instead of a superposition, we have a single energy eigenstate at $t = 0$. Fig. 1 shows the harmonic spectra for the cases when $|\psi\rangle(0)$ is equal to $|n = 1, l = 0, m = 0\rangle$, $|n = 2, l = 1, m = 0\rangle$ and $|n = 2, l = 1, m = -1\rangle$. Let us recall that

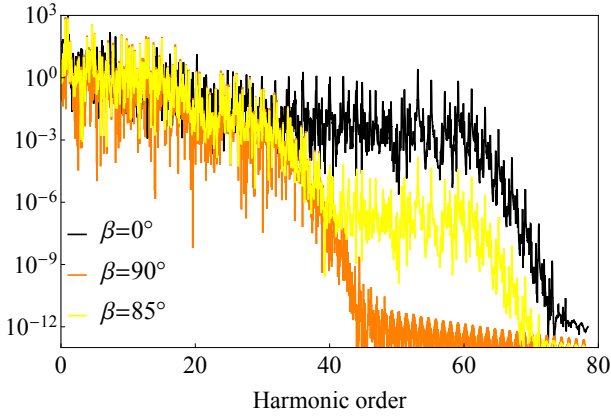


FIG. 3: HHG spectra for initial superpositions $\cos\beta|n=1, l=0, m=0\rangle + \sin\beta|n'=2, l'=1, m'=0\rangle$ for the values of β shown by the legend, and $\delta=0$. The parameters of the exciting field are the same as in Fig. 1.

the cutoff energy can be estimated as $E_c = I_p + 3.17 U_p$, where $U_p = e^2 E_0^2 / 4m\omega_0^2$ is the ponderomotive energy. I_p is the ionization potential for the ground state ($|\psi\rangle(0) = |1, 0, 0\rangle$). As a generalization, one might think that for excited states, I_p should be replaced by \tilde{I}_p , the energy difference between the initial state and the limit of the continuum. This is exactly what we can see in Fig. 1 for $|\psi\rangle(0) = |2, 1, 0\rangle$. However, for $|\psi\rangle(0) = |2, 1, -1\rangle$, we do not see a definite decrease of the cutoff frequency. The reason for this is the fact that the state $|2, 1, -1\rangle$ is dipole coupled to the ground state, thus during the time evolution the state $|1, 0, 0\rangle$ also gets populated. In other words, for $|\psi\rangle(0) = |2, 1, -1\rangle$, it is not the initial state the energy difference of which and the continuum determines the value of \tilde{I}_p . In fact, since a "downward" transition to the ground state is dipole-allowed, the value of \tilde{I}_p is undetermined, the dynamics populate various energy eigenstates, among which the ground state has the lowest energy. This is not the case for $|\psi\rangle(0) = |2, 1, 0\rangle$, since in this case there is no dipole-allowed transition to the ground state, and $\tilde{I}_p = I_p/2^2 (\approx 13.6\text{eV}/4$ for hydrogen).

Having understood the physical picture behind Fig. 1, we can conclude that our model can reproduce the most important features of the atomic HHG spectra. Therefore we can turn to the case when the initial states are proper superposition, i.e., β is neither 0 nor $\pi/2$ in Eq. (15). Figs. 2 and 3 show HHG spectra for different superpositions with $\delta=0$ in Eq. (15). For Fig. 2, the constituents of the superpositions are dipole coupled, unlike for Figs. 3, where $\langle 1, 0, 0 | D | 2, 1, 0 \rangle = 0$. The difference between the figures is clear: the effect of the initial atomic coherence is much stronger for the case of Fig. 3. As we have discussed above, for $|\psi\rangle(0) = |2, 1, -1\rangle$, the dynamics is unavoidably coupled to the ground state $|1, 0, 0\rangle$. Along this line, the combination of these two states as the initial superposition is not expected to strongly de-

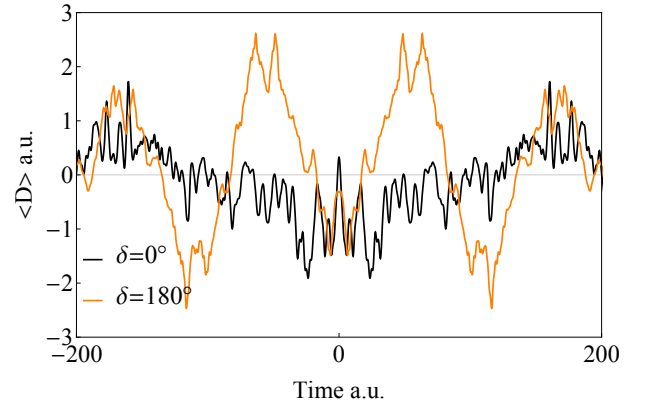


FIG. 4: The time dependence of the HHG signal for a superposition $\cos\beta|n=1, l=0, m=0\rangle + \sin\beta|n'=2, l'=1, m'=-1\rangle$ with $\beta=\pi/4$ and the indicated values of δ . The parameters of the exciting field are the same as in Fig. 1.

pend on the weight of the constituents, since these two states get mixed during the time evolution anyway.

On the other hand, when the constituents of the initial superposition are not dipole coupled, their dynamics follow separated "ladders" to the continuum and back again. This independence leads to the double cutoff structure seen in Fig. 3, where both of the cutoffs belonging to $|1, 0, 0\rangle$ and $|2, 1, 0\rangle$ are clearly visible when the initial state is the superposition of these states. (Note that $|2, 1, 0\rangle$ has to be dominant in order to see this structure, since when the weight of $|1, 0, 0\rangle$ is large enough, it produces observable signal also in the region between the "two cutoffs" and the double step-like behaviour of the spectra becomes less apparent on a logarithmic scale that is traditionally used for these plots.) Let us also note that a similar double cutoff structure was obtained in Ref. [26] using a different numerical approach. That is, although the constituents of the superposition of the states $|1, 0, 0\rangle$ and $|2, 1, 0\rangle$ essentially evolves as two independent states, their weights (determined by β in Eq. 15) create observable differences in the spectra.

The most sophisticated signature of quantum mechanical atomic coherence is the dependence of the dynamics on the relative phase δ that appears in Eq. (15). However, there is no δ dependence (neither in the spectra, nor in the time evolution of the dipole moment expectation values) for the superpositions of states $|1, 0, 0\rangle$ and $|2, 1, 0\rangle$. In order to understand this, we have to recall the constituents of these superpositions follow independent dynamics, and the dipole moment matrix element between them always vanishes. Therefore both $|1, 0, 0\rangle$ and $|2, 1, 0\rangle$ produce their HHG signal independently, and, in this sense, although the term $e^{i\delta}$ in Eq. (15) multiplies only $|2, 1, 0\rangle$, it plays the role of an overall, irrelevant phase factor. This is exactly what we have seen in our simulations.

On the other hand, for dipole coupled states, there is

a nonzero cross term $\langle 1, 0, 0 | D | 2, 1, -1 \rangle$ already at $t = 0$, and its nontrivial time evolution gives an observable contribution to the HHG spectra, as well as to the time dependent HHG signals. As an example, Fig. 4 shows the time dependent dipole moment expectation value for the same value of β , but for different phases δ in a superposition of these states. As we can see, the question whether the sign between the constituents of the initial superposition is $+$ or $-$ ($\delta = 0$ or π in the figure), plays a decisive role in the time evolution of the system. Generally, the positions, the heights as well as the widths of the peaks do depend on the value of δ , which can be controlled experimentally. The substantially different HHG signals seen in Fig. 4 point towards the control of high harmonic radiation by utilizing atomic coherence effects.

IV. SUMMARY

As it is known, Floquet theorem is an efficient method to solve the time-dependent Schrödinger equation for monochromatic excitation. Having expanded the corresponding equations in a Sturmian basis, we obtained a

method that is particularly suitable for the description of high-order harmonic generation (HHG) in hydrogen-like gases. The quantum mechanical coherence of the initial states were found to have strong influence on the HHG spectra. In more details, by considering superpositions of usual hydrogenic energy eigenstates as initial states, we have shown that the weights of the constituent states play an important role in the production of the high harmonic radiation. Moreover, for a linearly polarized exciting field, when the constituents of the initial superposition are dipole-coupled, the time-dependent HHG signal is shown to be also sensitive to the quantum mechanical phase difference between the constituents of the initial superpositions. This demonstrates that atomic coherence effects can control the properties of high harmonic radiation.

The ELI-ALPS project (Grants No. GOP-1.1.1-12/B-2012-000 and No. GINOP-2.3.6-15-2015-00001) is supported by the European Union and co-financed by the European Regional Development Fund. Our work was also supported by the European Social Fund under contract EFOP-3.6.2-16-2017-00005.

-
- [1] F. Krausz and M. Ivanov, “Attosecond physics,” *Rev. Mod. Phys.* **81**, 163–234 (2009).
 - [2] G. Farkas and C. Tóth, “Proposal for attosecond light pulse generation using laser induced multiple-harmonic conversion processes in rare gases,” *Physics Letters A* **168**, 447 – 450 (1992).
 - [3] P. Agostini and L. F. DiMauro, “The physics of attosecond light pulses,” *Reports on Progress in Physics* **67**, 813 (2004).
 - [4] A. McPherson, G. Gibson, H. Jara, U. Johann, T. S. Luk, I. A. McIntyre, K. Boyer, and C. K. Rhodes, “Studies of multiphoton production of vacuum-ultraviolet radiation in the rare gases,” *J. Opt. Soc. Am. B* **4**, 595–601 (1987).
 - [5] M. Ferray, A. L’Huillier, X. F. Li, L. A. Lompre, G. Mainfray, and C. Manus, “Multiple-harmonic conversion of 1064 nm radiation in rare gases,” *Journal of Physics B: Atomic, Molecular and Optical Physics* **21**, L31 (1988).
 - [6] U. Teubner and P. Gibbon, “High-order harmonics from laser-irradiated plasma surfaces,” *Rev. Mod. Phys.* **81**, 445–479 (2009).
 - [7] G. D. Tsakiris, K. Eidmann, J. Meyer-ter-Vehn, and F. Krausz, “Route to intense single attosecond pulses,” *New Journal of Physics* **8**, 19 (2006).
 - [8] S. Kahaly, S. Monchocé, H. Vincenti, T. Dzelzainis, B. Dromey, M. Zepf, P. Martin, and F. Quéré, “Direct observation of density-gradient effects in harmonic generation from plasma mirrors,” *Phys. Rev. Lett.* **110**, 175001 (2013).
 - [9] T. Baeva, S. Gordienko, and A. Pukhov, “Theory of high-order harmonic generation in relativistic laser interaction with overdense plasma,” *Phys. Rev. E* **74**, 046404 (2006).
 - [10] S. Ghimire, A. D. DiChiara, E. Sistrunk, P. Agostini, L. F. DiMauro, and D. A. Reis, “Observation of high-order harmonic generation in a bulk crystal,” *Nature Physics* **7**, 138–141 (2011).
 - [11] M. F. Ciappina, J. A. Pérez-Hernández, T. Shaaran, M. Lewenstein, M. Krüger, and P. Hommelhoff, “High-order-harmonic generation driven by metal nanotip photoemission: Theory and simulations,” *Phys. Rev. A* **89**, 013409 (2014).
 - [12] A. L’Huillier, K. J. Schafer, and K. C. Kulander, “Theoretical aspects of intense field harmonic generation,” *Journal of Physics B: Atomic, Molecular and Optical Physics* **24**, 3315 (1991).
 - [13] P. B. Corkum, “Plasma perspective on strong field multiphoton ionization,” *Phys. Rev. Lett.* **71**, 1994–1997 (1993).
 - [14] J. L. Krause, K. J. Schafer, and K. C. Kulander, “Calculation of photoemission from atoms subject to intense laser fields,” *Phys. Rev. A* **45**, 4998–5010 (1992).
 - [15] M. Lewenstein, P. Balcou, M. Y. Ivanov, A. L’Huillier, and P. B. Corkum, “Theory of high-harmonic generation by low-frequency laser fields,” *Phys. Rev. A* **49**, 2117–2132 (1994).
 - [16] G. Floquet, “Sur les quations différentielles linaires a coefficients priodiques,” *Ann. École Norm. Sup.* **12**, 46–88 (1883).
 - [17] R. M. Potvliege and R. Shakeshaft, “Multiphoton processes in an intense laser field: Harmonic generation and total ionization rates for atomic hydrogen,” *Phys. Rev. A* **40**, 3061–3079 (1989).
 - [18] F. H. M. Faisal and J. Z. Kamiński, “Floquet-bloch theory of high-harmonic generation in periodic structures,” *Phys. Rev. A* **56**, 748–762 (1997).
 - [19] V. Szaszó-Bogár, F. M. Peeters, and P. Földi, “Oscillating spin-orbit interaction in two-dimensional superlattices: Sharp transmission resonances and time-dependent spin-polarized currents,” *Phys. Rev. B* **91**, 235311 (2015).

- [20] O. Goscinski, “Preliminary research report no. 217, quantum chemistry group, uppsala university, (1968),” .
- [21] O. Goscinski, *Advances in Quantum Chemistry* **41**, 57–85 (2002).
- [22] C. Joachain, N. Kylstra, and R. Potvliege, *Atoms in Intense Laser Fields* (Cambridge University Press, 2012).
- [23] V. Ayadi, M. G.Benedict, P. Dombi, and P. Földi, “Atomic coherence effects in few-cycle pulse induced ionization,” *Eur. Phys. J. D* (2016) 70: 266. (2016).
- [24] J. Avery and J. Avery, *Generalized Sturmians and Atomic Spectra* (World Scientific, 2006).
- [25] P. Popelier, *Solving the Schrödinger Equation: Has Everything Been Tried?* (Imperial College Press, 2011).
- [26] J. B. Watson, A. Sanpera, X. Chen, and K. Burnett, “Harmonic generation from a coherent superposition of states,” *Phys. Rev. A* **53**, R1962–R1965 (1996).